Hindawi
Discrete Dynamics in Nature and Society
Volume 2024, Article ID 9185585, 18 pages
https://doi.org/10.1155/2024/9185585

Research Article

Analysis of the Dynamical Properties of Discrete Predator-Prey Systems with Fear Effects and Refuges

Wei Li, Chunrui Zhang, and Mi Wang

Department of Mathematics, Northeast Forestry University, Harbin 150040, China

Correspondence should be addressed to Chunrui Zhang; math@nefu.edu.cn

Received 23 January 2024; Revised 8 April 2024; Accepted 25 April 2024; Published 11 May 2024

Academic Editor: Marek Galewski

This paper examines the dynamic behavior of a particular category of discrete predator-prey system that feature both fear effect and refuge, using both analytical and numerical methods. The critical coefficients and properties of bifurcating periodic solutions for Flip and Hopf bifurcations are computed using the center manifold theorem and bifurcation theory. Additionally, numerical simulations are employed to illustrate the bifurcation phenomenon and chaos characteristics. The results demonstrate that period-doubling and Hopf bifurcations are two typical routes to generate chaos, as evidenced by the calculation of the maximum Lyapunov exponents near the critical bifurcation points. Finally, a feedback control method is suggested, utilizing feedback of system states and perturbation of feedback parameters, to efficiently manage the bifurcations and chaotic attractors of the discrete predator-prey model.

1. Introduction

In exploring population dynamics, continuum modelling is often used to explain population trends in situations where populations are large or where there are overlapping generations [1, 2]. However, when there is no overlap between generations of a population, the growth pattern of the population will show obvious stages and discontinuities. In this case, a discrete model can more accurately capture and reflect this discontinuity in population change. Discrete predator-prey systems can exhibit complex dynamical behavior, which has attracted many researchers to study them [3–6]. Zhang et al. [7] studied the dynamics of a discrete FitzHugh–Nagumo model by applying central manifold and normal form analysis and demonstrated that the system is capable of undergoing Neimark–Sacker and flip bifurcations even in the absence of diffusion. Li et al. [8] obtained rich dynamic properties by building a space-time discrete model with periodic boundary conditions. Therefore, discrete dynamical systems can have more complex dynamics, and their dynamic behavior can more closely approximate the complex dynamics of the phenomena represented by the model.

Since the biological population itself is a complex nonlinear system, this nonlinearity is the fundamental cause of the occurrence of chaos [9, 10]. Through the study of biological groups, we can see that there are many chaotic behaviors embedded in them [11]. Such chaotic phenomena are not limited to animal reproduction and evolution, such as competition and parasitism between the groups [12]. However, chaos in biological groups is not all good, and the negative chaotic situations that exist in nature can have a negative effect on human survival and development; therefore, controlling these chaotic situations is important for maintaining the stability of the ecosystem [13–17]. Discrete systems have two special bifurcations, flip bifurcation and Hopf bifurcation, which in turn are the two ways for discrete systems to move towards chaos. There are now many ways of controlling the chaos generated by the model: Vinoth et al. [18] describe three different approaches to chaos control: state feedback, pole placement, and hybrid control. Nowadays, nature, because of prolonged disturbances, has destroyed its natural rules of reproduction and put it on the verge of extinction, so it is important to carry out the study of chaos control of biological groups with important theoretical and practical application value.

Predator-prey interactions play a crucial role in the study of biological systems and population dynamics. Various examples have been explored, including populations with different functional response functions [19–24]. Additionally, the impact of having a refuge on population dynamics has been examined [25–28]. The reproductive capacity of prey populations is a vital factor in understanding population dynamics. The size of the prey population is influenced by the number of predators, which, in turn, is affected by the size of the prey population. Furthermore, the fear of predators among prey species significantly impacts the reproductive capacity of prey populations, thereby influencing the entire predation system. Wang et al. [29] proposed an expression $f(K, y) = (1/1 + Ky)$ to describe the effect of fear on prey populations, where the degree of fear is represented by K. This expression can be utilized to predict the size of the prey population, which ultimately affects the stability of the entire ecosystem. Fakhry et al. [30] proposed a square root prey-predator model with fear

$$\begin{cases} \dfrac{dx}{dt} = rx(1-x)\left(\dfrac{1}{1+Ky}\right) - y\sqrt{x}, \\ \dfrac{dy}{dt} = -\alpha y + \beta\sqrt{x}\, y, \end{cases} \tag{1}$$

with initial condition $x(t) > 0$ and $y(t) > 0$, where K indicates the level of fear, α indicates the death rate of the predator in the absence of prey, β indicates the conversion rate of prey to predator, and r is the growth rate of the prey.

In 2019, Zhang et al. [31] investigated predator-prey systems with fear effects and refuge

$$\begin{cases} \dfrac{dx}{dt} = \dfrac{\alpha x}{1+Ky} - bx^2 - \dfrac{\beta(1-m)xy}{1+a(1-m)x}, \\ \dfrac{dy}{dt} = -ry + \dfrac{c\beta(1-m)xy}{1+a(1-m)x}, \end{cases} \tag{2}$$

where K indicates the level of fear, α indicates the endowment growth rate of the bait, and r indicates the predator mortality rate. (β/a) indicates the maximum amount of predators eaten by each predator per unit of time, b indicates the coefficient of competition within the prey population, c indicates the conversion factor, and $(1-m)x$ indicates the amount of prey taken, $m \in [0, 1)$. The effects of fear and the impact of refuges on system stability are discussed. This model can better describe dynamic behaviors such as interactions and competition between species in ecosystems.

The discrete form of (2) can be obtained using Euler's method as follows:

$$\begin{cases} x_{n+1} = x_n + h\left(\dfrac{\alpha x_n}{1+Ky_n} - bx_n^2 - \dfrac{\beta(1-m)x_n y_n}{1+a(1-m)x_n}\right), \\ y_{n+1} = y_n + h\left(-ry_n + \dfrac{c\beta(1-m)x_n y_n}{1+a(1-m)x_n}\right). \end{cases} \tag{3}$$

This paper focuses on analyzing the model bifurcation and chaotic properties. In the first part, the existence and stability of the equilibrium point are discussed. In the second and third parts, the conditions for the existence of flip and Hopf bifurcation at the positive equilibrium point are considered, and the direction of the flip and Hopf bifurcation at the positive equilibrium point is derived by using the central manifold theorem. In the fourth part, the maximum Lyapunov exponent is used to discuss the occurrence of chaotic situations inside the system and to control the resulting chaotic situations, and finally, numerical simulations verify the correctness of the theoretical proofs.

2. Existence and Stability of Equilibrium Points

It is evident that system (3) possesses a trivial equilibrium point $N_0(0, 0)$ and a boundary equilibrium point $N_1(\alpha/b, 0)$.

Assuming (H_1): $c\beta - ar > 0$

If (H_1) holds, the only positive equilibrium point of the system can be obtained as $N^*(x^*, y^*)$, where $x^* = r/(c\beta - ar)(1-m)$, $y^* = 1/2K(\sqrt{\Delta} - 1 - \mathrm{Kcbr}/(1-m)^2(c\beta - ar)^2)$, $\Delta = (1 - \mathrm{Kcbx}^*/(1-m)(c\beta - ar))^2 + (4Kc\alpha/(1-m)(c\beta - ar))$.

The Jacobi matrix $J(\overline{x}, \overline{y})$ of system (3) at any equilibrium point is given by

$$J(\overline{x}, \overline{y}) = \begin{pmatrix} 1 + h\left(\dfrac{\alpha}{1+Ky} - 2bx - \dfrac{\beta(1-m)y}{(1+a(1-m)x)^2}\right) & -h\left(\dfrac{K\alpha x}{(1+Ky)^2} + \dfrac{\beta(1-m)x}{1+a(1-m)x}\right) \\ \dfrac{hc\beta(1-m)y}{(1+a(1-m)x)^2} & 1 + h\left(-r + \dfrac{c\beta(1-m)x}{1+a(1-m)x}\right) \end{pmatrix}\Bigg|_{(\overline{x},\overline{y})}. \tag{4}$$

To investigate the stability analysis of the equilibrium point of system (3), we present the following lemma. By utilizing the connections between the coefficients and roots of a quadratic equation [32], one can readily derive the following results.

Lemma 1. *Assume that* $F(\lambda) = \lambda^2 - A\lambda + B$ *and* $F(1) > 0$ *with* λ_1, λ_2 *are roots of* $F(\lambda) = 0$. *Then, the following results hold true:*

(i) $|\lambda_1| < 1$ *and* $|\lambda_2| < 1$ *if and only if* $F(-1) > 0$, $B < 1$.

(ii) $|\lambda_1| < 1$ *and* $|\lambda_2| > 1$, *or* $|\lambda_1| > 1$ *and* $|\lambda_2| < 1$ *if and only if* $F(-1) < 0$.

(iii) $|\lambda_1| > 1$ *and* $|\lambda_2| > 1$ *if and only if* $F(-1) < 0$, $B > 1$.

(iv) λ_1 *and* λ_2 *are complex and* $|\lambda_1| = 1$, $|\lambda_2| = 1$ *if and only if* $A^2 - 4B < 0$ *and* $B = 1$.

Theorem 2. *For the trivial equilibrium point* $N_0(0,0)$, *the characteristic equation of system (3) at* $N_0(0,0)$ *has two eigenvalues,* $\lambda_1 = 1 + h\alpha$ *and* $\lambda_2 = 1 - hr$

(i) If $h < 2/r$, *then* $|\lambda_1| > 1$, $|\lambda_2| < 1$, $N_0(0,0)$ *is a saddle point.*

(ii) If $h > 2/r$, *then* $|\lambda_1| > 1$, $|\lambda_2| > 1$, $N_0(0,0)$ *is a source.*

Theorem 3. *For the boundary equilibrium point* $N_1(\alpha/b, 0)$, *the characteristic equation of system (3) at* $N_1(\alpha/b, 0)$ *has the eigenvalue* $\lambda_1 = 1 - h\alpha$, $\lambda_2 = 1 + h(-r + c\beta(1-m)\alpha/b + a(1-m)\alpha)$, *let* $l = (c\beta - a\alpha)(1-m)$

(i) If $\begin{cases} l < br/\alpha \\ 0 < h < \min\{2/\alpha, -2b - 2a\alpha(1-m)/-br + \alpha l\} \end{cases}$, *then* $|\lambda_1| < 1$, $|\lambda_2| < 1$, $N_1(\alpha/b, 0)$ *is a sink.*

(ii) If $\begin{cases} l < br/\alpha \\ (2/\alpha) < h < -2b - 2a\alpha(1-m)/-br + \alpha l \end{cases}$, *then* $|\lambda_1| > 1$, $|\lambda_2| < 1$, *or if* $\begin{cases} l < br/\alpha \\ -2b - 2a\alpha(1-m)/-br + \alpha l < h < 2/\alpha \end{cases}$, *then* $|\lambda_1| < 1$, $|\lambda_2| > 1$, $N_1(\alpha/b, 0)$ *is a saddle point.*

(iii) If $\begin{cases} l < br/\alpha \\ h > \max\{2/\alpha, -2b - 2a\alpha(1-m)/-br + \alpha l\} \end{cases}$ *or* $\begin{cases} l > br/\alpha \\ h > 2/\alpha \end{cases}$, *then* $|\lambda_1| > 1$, $|\lambda_2| > 1$, $N_1(\alpha/b, 0)$ *is a source.*

For the point $N^*(x^*, y^*)$, we have

$$J(x^*, y^*) = \begin{pmatrix} 1 + h\left(\dfrac{2\alpha l^2}{(1+\sqrt{\Delta})l^2 - Kbcr}\right) + h\left(-\dfrac{2br}{l} - \dfrac{l(c\beta - ar)}{c^2\beta}\right) & -h\left(\dfrac{4K\alpha r l^3}{(1+\sqrt{\Delta})l^2 - Kbcr}\right) + \dfrac{hr}{c} \\ \dfrac{hc\beta(1-m)\left((\sqrt{\Delta}-1)l^2 - \mathrm{Kbcr}\right)}{2K(l + \alpha(1-m)r)^2} & 1 \end{pmatrix}. \quad (5)$$

Furthermore, the characteristic polynomial of $J(\overline{x}, \overline{y})$ when evaluated at the equilibrium point $N^*(x^*, y^*)$ can be expressed as follows:

$$f(\lambda) = \lambda^2 - (J_{11}(N^*) + 1)\lambda + J_{11}(N^*) - J_{12}(N^*)J_{21}(N^*), \quad (6)$$

where $J_{11}(N^*) = 1 + h(2\alpha l^2/(1+\sqrt{\Delta})l^2 - Kbcr) + h(-2br/l - l(c\beta - ar)/c^2\beta)$, $J_{12}(N^*) = -h(4K\alpha r l^3/(1+\sqrt{\Delta})l^2 - Kbcr) + hr/c$, $J_{21}(N^*) = hc\beta(1-m)((\sqrt{\Delta}-1)l^2 - Kbcr)/2K(l + \alpha(1-m)r)^2$, $J_{22}(N^*) = 1$.

Theorem 4. *For the point* $N^*(x^*, y^*)$

(i) If $\begin{cases} -J_{12}(N^*)J_{21}(N^*) > 0 \\ 2 + 2J_{11}(N^*) - J_{12}(N^*)J_{21}(N^*) > 0 \\ 1 - J_{11}(N^*) - J_{12}(N^*)J_{21}(N^*) > 0 \end{cases}$, *then* $|\lambda_1| < 1$, $|\lambda_2| < 1$, $N^*(x^*, y^*)$ *is a sink.*

(ii) If $\begin{cases} -J_{12}(N^*)J_{21}(N^*) > 0 \\ 2 + 2J_{11}(N^*) - J_{12}(N^*)J_{21}(N^*) < 0 \end{cases}$, *then* $|\lambda_1| < 1$ *and* $|\lambda_2| > 1$, *or* $|\lambda_1| > 1$ *and* $|\lambda_2| < 1$, $N^*(x^*, y^*)$ *is a saddle point.*

(iii) If $\begin{cases} -J_{12}(N^*)J_{21}(N^*) > 0 \\ 2 + 2J_{11}(N^*) - J_{12}(N^*)J_{21}(N^*) > 0 \\ 1 - J_{11}(N^*) - J_{12}(N^*)J_{21}(N^*) < 0 \end{cases}$, *then* $|\lambda_1| > 1$ *and* $|\lambda_2| > 1$, $N^*(x^*, y^*)$ *is a source.*

(iv) If $\begin{cases} J_{11}(N^*) - J_{12}(N^*)J_{21}(N^*) = 1 \\ (J_{11}(N^*) - 1)^2 + 4J_{12}(N^*)J_{21}(N^*) < 0 \end{cases}$, *then* λ_1, λ_2 *is a pair of conjugate complex roots.*

To validate the accuracy of the theoretical proof, numerical simulations are conducted in the following sections. When the parameters are taken as $h = 0.1, c = 0.9, r = 0.1$, $b = 0.01, d = 0.82146, e = 0.9, a = 0.5$, $K = 34.555, m = 0.89$, Theorem 4 of (i) is satisfied, see Figure 1.

With other parameters are kept constant, let $K = 15$, through the image can be obtained when the degree of fear is different, the final stability of the system is different, see Figure 2.

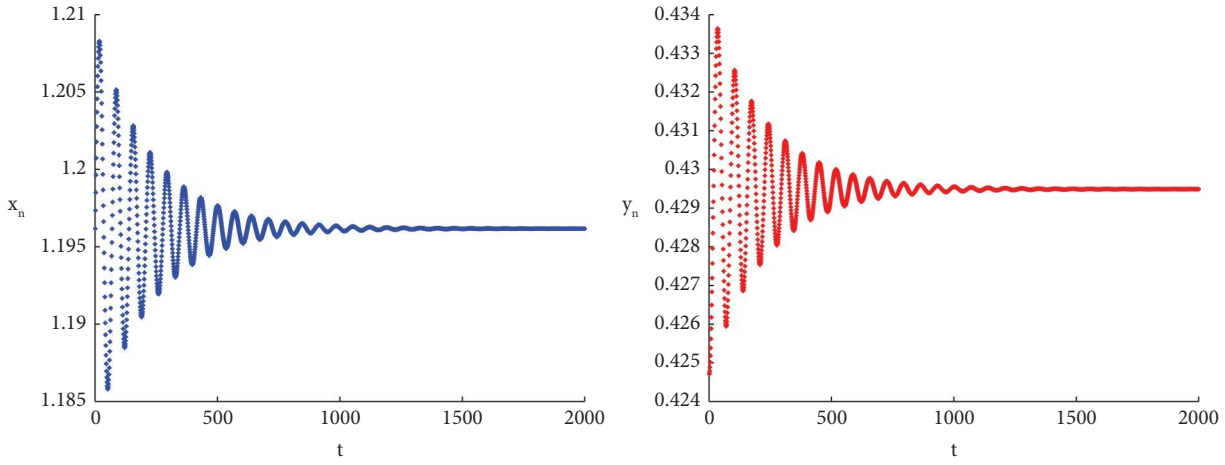

FIGURE 1: Equilibrium solution at $N^*(x^*, y^*) \approx (1.19617, 0.4247)$ when the parameters are taken as $h = 0.1$, $c = 0.9$, $r = 0.1$, $b = 0.01$, $d = 0.82146$, $e = 0.9$, $a = 0.5$, $K = 34.555$, and $m = 0.89$.

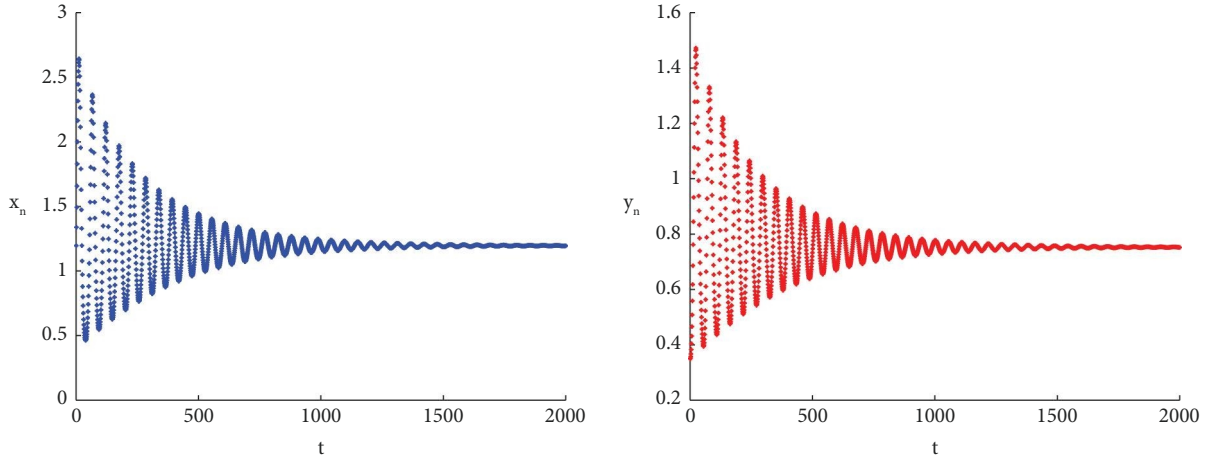

FIGURE 2: Equilibrium solution at $N^*(x^*, y^*) \approx (1.19617, 0.3497)$ when the parameters are taken as $h = 0.1$, $c = 0.9$, $r = 0.1$, $b = 0.01$, $d = 0.82146$, $e = 0.9$, $a = 0.5$, $K = 12$, and $m = 0.89$.

3. Flip Bifurcation at Positive Equilibrium Point

3.1. Conditions for the Existence of Flip Bifurcation. To obtain the bifurcation parameters, consider the transformations $\overline{x_{n+1}} = x_{n+1} - x^*$, $\overline{y_{n+1}} = y_{n+1} - y^*$, system (3) can be approximated as

$$\begin{cases} \overline{x_{n+1}} = \overline{x_n} + h\left(\dfrac{\alpha(\overline{x_n} + x^*)}{1 + K(\overline{y_n} + y^*)} - b(\overline{x_n} + x^*)^2 - \dfrac{\beta(1-m)(\overline{x_n} + x^*)(\overline{y_n} + y^*)}{1 + a(1-m)(\overline{x_n} + x^*)}\right), \\ \overline{y_{n+1}} = \overline{y_n} + h\left(-r(\overline{y_n} + y^*) + \dfrac{c\beta(1-m)(\overline{x_n} + x^*)(\overline{y_n} + y^*)}{1 + a(1-m)(\overline{x_n} + x^*)}\right). \end{cases} \tag{7}$$

Using the Taylor expansion at the point x^*, y^* yields the following expression:

$$\begin{pmatrix} \overline{x_{n+1}} \\ \overline{y_{n+1}} \end{pmatrix} = J\Big|_{(x^*,y^*)} \begin{pmatrix} \overline{x_n} \\ \overline{y_n} \end{pmatrix} + h \begin{pmatrix} \psi_1(\overline{x_n}, \overline{y_n}) \\ \psi_2(\overline{x_n}, \overline{y_n}) \end{pmatrix},$$
$$\psi_1(\overline{x_n}, \overline{y_n}) = z_1\overline{x_n}^2 + z_2\overline{x_n y_n} + z_3\overline{y_n}^2 + z_4\overline{x_n}^3 + z_5\overline{x_n}^2\overline{y_n} + z_6\overline{x_n y_n}^2 + z_7\overline{y_n}^3 + O\left(\left(|\overline{x_n}| + |\overline{y_n}|\right)^4\right), \tag{8}$$
$$\psi_2(\overline{x_n}, \overline{y_n}) = u_1\overline{x_n}^2 + u_2\overline{x_n y_n} + u_3\overline{x_n}^3 + u_5\overline{x_n}^2\overline{y_n} + O\left(\left(|\overline{x_n}| + |\overline{y_n}|\right)^4\right),$$

where $z_1 = -b + ((1-m)^2 a\beta y^*/(1+ax^*(1-m))^3)$, $z_2 = -(K\alpha/(1+Ky^*)^2) - (\beta(1-m)/(1+x^*a(1-m))^2)$, $z_3 = (K^2\alpha x^*/(1+Ky^*)^3)$, $z_4 = -(y^*a^2\beta(1-m)^3/(1+x^*a(1-m))^4)$, $z_5 = (a(1-m)^2\beta/(1+x^*a(1-m))^3)$, $z_6 = (K^2\alpha/(1+Ky^*)^3)$, $z_7 = (K^3\alpha x^*/(1+Ky^*)^4)$, $u_1 = -(cy^*a\beta(1-m)^2/(1+x^*a(1-m))^3)$, $u_2 = (c\beta(1-m)/(1+x^*a(1-m))^2)$, $u_3 = (c(1-m)^3a^2\beta y^*/(1+ax^*(1-m))^4)$, $u_4 = 0$, $u_5 = -(ca\beta(1-m)^2/(1+x^*a(1-m))^3)$.

According to the characteristic polynomial (6), we can get

$$f(-1) = 2 + 2J_{11}(N^*) - J_{12}(N^*)J_{21}(N^*) = 0. \tag{9}$$

Since the step size $h > 0$, it is possible to obtain the branching value $h^* = (d_2 + \sqrt{d_2^2 - 16d_1}/2d_1)$. Here, $d_1 = (4K\alpha rl^3 c\beta(1-m)/2K(l+a(1-m)r)^2) + (r((1+\sqrt{\Delta})l^2 - Kbcr)c\beta(1-m)/2cK(l+a(1-m)r)^2)$, $d_2 = (4l^2\alpha/(1+\sqrt{\Delta})l^2 - Kbcr) - (4br/l) - (2l^2/c^2\beta(1-m))$

Let $h = h^* + \delta$. We consider δ as a small bifurcation parameter, and the perturbation of system (7) can be described by the following system, where $|\delta| \ll 1$.

$$\begin{pmatrix} \overline{x_{n+1}} \\ \overline{y_{n+1}} \end{pmatrix} = \begin{pmatrix} 1 + (h^*+\delta)L & -(h^*+\delta)\dfrac{4K\alpha rl^3}{i_2} + \dfrac{r}{c} \\ \dfrac{(h^*+\delta)c\beta(1-m)i_1}{i_3} & 1 \end{pmatrix} \begin{pmatrix} \overline{x_n} \\ \overline{y_n} \end{pmatrix} + (h^*+\delta) \begin{pmatrix} \psi_1(\overline{x_n}, \overline{y_n}) \\ \psi_2(\overline{x_n}, \overline{y_n}) \end{pmatrix}, \tag{10}$$

where $L = ((2\alpha l^2/i_2) - (2br/l) - (\beta(1-m)i_1/i_3))$, $i_1 = (\sqrt{\Delta} - 1)l^2 - Kbcr$, $i_2 = (1+\sqrt{\Delta})l^2 - Kbcr$, and $i_3 = 2K(l+\alpha(1-m)r)^2$.

In this case the characteristic polynomial (7) can be rewritten as

$$g(\lambda) = \lambda^2 - (2 + (h^*+\delta)L)\lambda + 1 + (h^*+\delta)L + (h^*+\delta)^2\left(\frac{4K\alpha rl^3}{i_2} + \frac{r}{c}\right)\left(\frac{c\beta(1-m)i_1}{i_3}\right), \tag{11}$$

solve for

$$\lambda_1 = \frac{1}{2}\left(2 + L\delta + Lh^* - \frac{\sqrt{(\delta+h^*)^2\left(-16cKl^3r\alpha i_1\beta(1-m) + i_2\left(L^2i_3 - 4ri_1\beta(1-m)\right)\right)}}{\sqrt{i_2 i_3}}\right),$$
$$\lambda_2 = \frac{1}{2}\left(2 + L\delta + Lh^* + \frac{\sqrt{(\delta+h^*)^2\left(-16cKl^3r\alpha i_1\beta(1-m) + i_2\left(L^2i_3 - 4ri_1\beta(1-m)\right)\right)}}{\sqrt{i_2 i_3}}\right). \tag{12}$$

The transversal condition at $N^*(x^*, y^*)$ is

$$\left.\frac{d\lambda_{1,2}}{d\delta}\right|_{\delta=0} = \frac{1}{2}\left(L \pm \frac{\sqrt{h^{*2}\left(-16cKl^3r\alpha i_1\beta(1-m)+i_2\left(L^2i_3-4ri_1\beta(1-m)\right)\right)}}{\sqrt{i_2i_3}\,h^*}\right). \tag{13}$$

If $(d\lambda_{1,2}/d\delta)|_{\delta=0}|_{\delta=0} \neq 0$, flip bifurcation occurs at the positive equilibrium point $N^*(x^*, y^*)$.

3.2. The Normal Form of Flip Bifurcation Solutions. Define

$$A = \begin{pmatrix} 1+h^*L & -h^*\dfrac{4K\alpha rl^3}{i_2}+\dfrac{r}{c} \\ \dfrac{h^*c\beta(1-m)i_1}{i_3} & 1 \end{pmatrix}. \tag{14}$$

If the eigenvalue of A is $\lambda = -1$, then the corresponding eigenvector is

$$T_1 = \begin{pmatrix} -h^*\dfrac{4K\alpha rl^3}{i_2}+\dfrac{r}{c} \\ -2-h^*L \end{pmatrix}. \tag{15}$$

If the eigenvalue of A is $\lambda = \lambda_2$, then the corresponding eigenvector is

$$T_2 = \begin{pmatrix} -h^*\dfrac{4K\alpha rl^3}{i_2}+\dfrac{r}{c} \\ \lambda_2-1-h^*L \end{pmatrix}. \tag{16}$$

Then the following invertible matrix can be obtained:

$$T = \begin{pmatrix} T_1 & T_2 \end{pmatrix} = \begin{pmatrix} -h^*\dfrac{4K\alpha rl^3}{i_2}+\dfrac{r}{c} & -h^*\dfrac{4K\alpha rl^3}{i_2}+\dfrac{r}{c} \\ -2-h^*L & \lambda_2-1-h^*L \end{pmatrix}. \tag{17}$$

Using the transformation $\begin{pmatrix} N_n \\ P_n \end{pmatrix} = T^{-1}\begin{pmatrix} \overline{x_n} \\ \overline{y_n} \end{pmatrix}$, system (7) is transformed into

$$\begin{pmatrix} N_{n+1} \\ P_{n+1} \end{pmatrix} = \begin{pmatrix} -1 & 0 \\ 0 & \lambda_2 \end{pmatrix}\begin{pmatrix} N_n \\ P_n \end{pmatrix} + \begin{pmatrix} f_1\left(\overline{x_n}, \overline{y_n}, \delta\right) \\ f_2\left(\overline{x_n}, \overline{y_n}, \delta\right) \end{pmatrix},$$

$$\begin{aligned} f_1\left(\overline{x_n}, \overline{y_n}, \delta\right) &= a_{11}\overline{x_n}\delta + a_{12}\overline{y_n}\delta + b_{11}\overline{x_n}^2 + b_{12}\overline{x_ny_n} + b_{13}\overline{y_n}^2 + b_{14}\overline{x_n}^3 + b_{15}\overline{x_n}^2\overline{y_n} + b_{16}\overline{x_n}\overline{y_n}^2 + b_{17}\overline{y_n}^3 \\ &\quad + c_{11}\overline{x_n}^2\delta + c_{12}\overline{x_ny_n}\delta + c_{13}\overline{y_n}^2\delta + c_{14}\overline{x_n}^3\delta + c_{15}\overline{x_n}^2\overline{y_n}\delta + c_{16}\overline{x_n}\overline{y_n}^2\delta + c_{17}\overline{y_n}^3\delta, \\ f_2\left(\overline{x_n}, \overline{y_n}, \delta\right) &= a_{21}\overline{x_n}\delta + a_{22}\overline{y_n}\delta + b_{21}\overline{x_n}^2 + b_{22}\overline{x_ny_n} + b_{23}\overline{y_n}^2 + b_{24}\overline{x_n}^3 + b_{25}\overline{x_n}^2\overline{y_n} + b_{26}\overline{x_n}\overline{y_n}^2 \\ &\quad + b_{27}\overline{y_n}^3 + c_{21}\overline{x_n}^2\delta + c_{22}\overline{x_ny_n}\delta + c_{23}\overline{y_n}^2\delta + c_{24}\overline{x_n}^3\delta + c_{25}\overline{x_n}^2\overline{y_n}\delta + c_{26}\overline{x_n}\overline{y_n}^2\delta + c_{27}\overline{y_n}^3\delta, \end{aligned} \tag{18}$$

where

$$
\begin{aligned}
a_{11} &= \frac{ci_2\left(-1+\lambda_2-Lh^*\right)}{r\left(i_2-4cKl^3\alpha h^*\right)\left(1+\lambda_2\right)}\left(-2bx^*+\frac{(-1+m)\beta y^*}{\left(-1+a(-1+m)x^*\right)^2}+\frac{\alpha}{1+Ky^*}\right)-\frac{cy^*\beta(-1+m)}{\left(1+\lambda_2\right)\left(1+a(-1+m)x^*\right)^2},\\
a_{12} &= \frac{cx^*i_2\left(-1+\lambda_2-Lh^*\right)}{r\left(i_2-4cKl^3\alpha h^*\right)\left(1+\lambda_2\right)}\left(\frac{(-1+m)\beta}{1+(a-am)x^*}-\frac{K\alpha}{\left(1+Ky^*\right)^2}\right)-\frac{cx^*\beta(-1+m)}{\left(1+\lambda_2\right)\left(1+a(-1+m)x^*\right)},\\
b_{11} &= -\frac{ci_2\left(1-\lambda_2+Lh^*\right)}{r\left(1+\lambda_2\right)\left(i_2-4cKl^3\alpha h^*\right)}z_1+\frac{4cKl^3r\alpha h^*-ri_2}{r\left(1+\lambda_2\right)\left(i_2-4cKl^3\alpha h^*\right)}u_1,\\
b_{12} &= -\frac{ci_2\left(1-\lambda_2+Lh^*\right)}{r\left(1+\lambda_2\right)\left(i_2-4cKl^3\alpha h^*\right)}z_2+\frac{4cKl^3r\alpha h^*-ri_2}{r\left(1+\lambda_2\right)\left(i_2-4cKl^3\alpha h^*\right)}u_2,\\
b_{13} &= \frac{ci_2\left(-1+\lambda_2-Lh^*\right)}{r\left(1+\lambda_2\right)\left(i_2-4cKl^3\alpha h^*\right)}z_3,\\
b_{14} &= -\frac{ci_2\left(1-\lambda_2+Lh^*\right)}{r\left(1+\lambda_2\right)\left(i_2-4cKl^3\alpha h^*\right)}z_4+\frac{4cKl^3r\alpha h^*-ri_2}{r\left(1+\lambda_2\right)\left(i_2-4cKl^3\alpha h^*\right)}u_3,\\
b_{15} &= -\frac{ci_2\left(1-\lambda_2+Lh^*\right)}{r\left(1+\lambda_2\right)\left(i_2-4cKl^3\alpha h^*\right)}z_5+\frac{4cKl^3r\alpha h^*-ri_2}{r\left(1+\lambda_2\right)\left(i_2-4cKl^3\alpha h^*\right)}u_5,\\
b_{16} &= \frac{ci_2\left(-1+\lambda_2-Lh^*\right)}{r\left(1+\lambda_2\right)\left(i_2-4cKl^3\alpha h^*\right)}z_6,\\
b_{17} &= \frac{ci_2\left(-1+\lambda_2-Lh^*\right)}{r\left(1+\lambda_2\right)\left(i_2-4cKl^3\alpha h^*\right)}z_7,\\
a_{21} &= \frac{(-1+m)\left(2+Lh^*\right)ci_2\beta y^*}{r\left(i_2-4cKl^3\alpha h^*\right)\left(1+\lambda_2\right)\left(-1+a(-1+m)x^*\right)^2}+\frac{\alpha ci_2\left(2+Lh^*\right)}{r\left(i_2-4cKl^3\alpha h^*\right)\left(1+\lambda_2\right)\left(1+Ky^*\right)}\\
&\quad+\frac{cy^*\beta(-1+m)}{\left(1+\lambda_2\right)\left(1+a(-1+m)x^*\right)^2}-\frac{2bx^*\left(ci_2\left(2+Lh^*\right)\right)}{r\left(i_2-4cKl^3\alpha h^*\right)\left(1+\lambda_2\right)},\\
a_{22} &= \frac{(-1+m)cx^*\beta}{\left(1+a(-1+m)x^*\right)\left(1+\lambda_2\right)}+\frac{(-1+m)cx^*\beta i_2\left(2+Lh^*\right)}{r\left(i_2-4cKl^3\alpha h^*\right)\left(1+\lambda_2\right)\left(1+a(-1+m)x^*\right)}\\
&\quad-\frac{Kcx^*\alpha i_2\left(2+Lh^*\right)}{r\left(i_2-4cKl^3\alpha h^*\right)\left(1+\lambda_2\right)\left(1+Ky^*\right)^2},\\
b_{21} &= \frac{ci_2\left(2+Lh^*\right)}{r\left(1+\lambda_2\right)\left(i_2-4cKl^3\alpha h^*\right)}z_1+\frac{-4cKl^3r\alpha h^*+ri_2}{r\left(1+\lambda_2\right)\left(i_2-4cKl^3\alpha h^*\right)}u_1,\\
b_{22} &= \frac{ci_2\left(2+Lh^*\right)}{r\left(1+\lambda_2\right)\left(i_2-4cKl^3\alpha h^*\right)}z_2+\frac{-4cKl^3r\alpha h^*+ri_2}{r\left(1+\lambda_2\right)\left(i_2-4cKl^3\alpha h^*\right)}u_2,\\
b_{23} &= \frac{ci_2\left(2+Lh^*\right)}{r\left(1+\lambda_2\right)\left(i_2-4cKl^3\alpha h^*\right)}z_3,\\
b_{24} &= \frac{ci_2\left(2+Lh^*\right)}{r\left(1+\lambda_2\right)\left(i_2-4cKl^3\alpha h^*\right)}z_4+\frac{-4cKl^3r\alpha h^*+ri_2}{r\left(1+\lambda_2\right)\left(i_2-4cKl^3\alpha h^*\right)}u_3,\\
b_{25} &= \frac{ci_2\left(2+Lh^*\right)}{r\left(1+\lambda_2\right)\left(i_2-4cKl^3\alpha h^*\right)}z_5+\frac{-4cKl^3r\alpha h^*+ri_2}{r\left(1+\lambda_2\right)\left(i_2-4cKl^3\alpha h^*\right)}u_5,\\
b_{26} &= \frac{ci_2\left(2+Lh^*\right)}{r\left(1+\lambda_2\right)\left(i_2-4cKl^3\alpha h^*\right)}z_6,\\
b_{27} &= \frac{ci_2\left(2+Lh^*\right)}{r\left(1+\lambda_2\right)\left(i_2-4cKl^3\alpha h^*\right)}z_7,\\
b_{ij} &= h^*c_{ij}, \quad (i=1,2;\ j=1,2,\ldots,7).
\end{aligned}
\tag{19}
$$

Using the transformation $\begin{pmatrix} \overline{x_{n+1}} \\ \overline{y_{n+1}} \end{pmatrix} = T\begin{pmatrix} N_{n+1} \\ P_{n+1} \end{pmatrix}$, system (10) becomes

$$\begin{pmatrix} N_{n+1} \\ P_{n+1} \end{pmatrix} = \begin{pmatrix} -N_n \\ \lambda_2 P_n \end{pmatrix} + \begin{pmatrix} f_3(N_n, P_n, \delta) \\ f_4(N_n, P_n, \delta) \end{pmatrix},$$
$$\begin{aligned} f_3(N_n, P_n, \delta) &= d_{11}N_n\delta + d_{12}P_n\delta + e_{11}N_n^2 + e_{12}N_nP_n + e_{13}P_n^2 + e_{14}N_n^3 + e_{15}N_n^2P_n + e_{16}N_nP_n^2 + e_{17}P_n^3 + f_{11}N_n^2\delta \\ &\quad + f_{12}N_nP_n\delta + f_{13}P_n^2\delta + f_{14}P_n^3\delta + f_{15}N_n^2p\delta + f_{16}N_nP_n^2\delta + f_{17}P_n^3\delta, \\ f_4(N_n, P_n, \delta) &= d_{21}N_n\delta + d_{22}P_n\delta + e_{21}N_n^2 + e_{22}N_nP_n + e_{23}P_n^2 + e_{24}N_n^3 + e_{25}N_n^2P_n + e_{26}N_nP_n^2 + e_{27}P_n^3 + f_{21}N_n^2\delta \\ &\quad + f_{22}N_nP_n\delta + f_{23}P_n^2\delta + f_{24}P_n^3\delta + f_{25}N_n^2p\delta + f_{26}N_nP_n^2\delta + f_{27}P_n^3\delta, \end{aligned} \tag{20}$$

let

$$k_{11} = k_{21} = -h^*\frac{4K\alpha rl^3}{i_2} + \frac{r}{c}, k_{12} = -2 - \mathrm{L}, k_{22} = \lambda_2 - 1 - \mathrm{L}, \tag{21}$$

then

$$\begin{aligned} &d_{11} = a_{11}k_{11} + a_{12}k_{21}, d_{12} = a_{11}k_{12} + a_{12}k_{22}, \\ &e_{11} = b_{11}k_{11}^2 + b_{12}k_{11}k_{21} + b_{13}k_{21}^2, \\ &e_{12} = 2b_{11}k_{11}k_{12} + b_{12}(k_{11}k_{22} + k_{12}k_{21}) + 2b_{13}k_{21}k_{22}, \\ &e_{13} = b_{11}k_{12}^2 + b_{12}k_{12}k_{22} + b_{13}k_{22}^2, e_{14} = b_{14}k_{11}^3 + b_{15}k_{11}^2k_{21} + b_{16}k_{11}k_{21}^2 + b_{17}k_{21}^3, \\ &e_{15} = 3b_{14}k_{11}^2k_{12} + b_{15}\left(k_{11}^2k_{22} + 2k_{11}k_{12}k_{21}\right) + b_{16}\left(2k_{11}k_{21}k_{22} + k_{12}k_{21}^2\right) + 3b_{17}k_{21}^2k_{22}, \\ &e_{16} = 3b_{14}k_{11}k_{12}^2 + b_{15}\left(2k_{11}k_{12}k_{22} + k_{12}^2k_{21}\right) + b_{16}\left(k_{11}k_{22}^2 + 2k_{12}k_{21}k_{22}\right) + 3b_{17}k_{21}k_{22}^2, \\ &e_{17} = b_{14}k_{12}^3 + b_{15}k_{12}^2k_{22} + b_{16}k_{12}k_{22}^2 + b_{17}k_{22}^3, \\ &d_{21} = a_{21}k_{11} + a_{22}k_{21}, d_{22} = a_{21}k_{12} + a_{22}k_{22}, \\ &e_{21} = b_{21}k_{11}^2 + b_{22}k_{11}k_{21} + b_{23}k_{21}^2, \\ &e_{22} = 2b_{21}k_{11}k_{12} + b_{22}(k_{11}k_{22} + k_{12}k_{21}) + 2b_{23}k_{21}k_{22}, \\ &e_{23} = b_{21}k_{12}^2 + b_{22}k_{12}k_{22} + b_{23}k_{22}^2, e_{24} = b_{24}k_{11}^3 + b_{25}k_{11}^2k_{21} + b_{26}k_{11}k_{21}^2 + b_{27}k_{21}^3, \\ &e_{25} = 3b_{24}k_{11}^2k_{12} + b_{25}\left(k_{11}^2k_{22} + 2k_{11}k_{12}k_{21}\right) + b_{26}\left(2k_{11}k_{21}k_{22} + k_{12}k_{21}^2\right) + 3b_{27}k_{21}^2k_{22}, \\ &e_{26} = 3b_{24}k_{11}k_{12}^2 + b_{25}\left(2k_{11}k_{12}k_{22} + k_{12}^2k_{21}\right) + b_{26}\left(k_{11}k_{22}^2 + 2k_{12}k_{21}k_{22}\right) + 3b_{27}k_{21}k_{22}^2, \\ &e_{27} = b_{24}k_{12}^3 + b_{25}k_{12}^2k_{22} + b_{26}k_{12}k_{22}^2 + b_{27}k_{22}^3, \\ &e_{ij} = h^*f_{ij}, \quad (i = 1, 2; j = 1, 2, \ldots, 7). \end{aligned} \tag{22}$$

During our analysis, we will utilize the central manifold theorem and normal form theory to investigate the direction of the flip bifurcation at the point $N^*(x^*, y^*)$.

Let

$$\theta_1 = \left(\frac{\partial^2 f}{\partial \widetilde{N_n}\partial\delta} + \frac{1}{2}\frac{\partial f}{\partial\delta}\frac{\partial^2 f}{\partial \widetilde{N}_n^2}\right)\Big|_{(0,0)}, \theta_2 = \left(\frac{1}{6}\frac{\partial^3 f}{\partial \widetilde{N}_n^3} + \left(\frac{1}{2}\frac{\partial^2 f}{\partial \widetilde{N}_n^2}\right)^2\right)\Big|_{(0,0)}, \tag{23}$$

where the coefficients of θ_1 and θ_2 are derived from (20).

Theorem 5. *The system exhibits a flip bifurcation at the immobile point $N^*(x^*, y^*)$ if both θ_1 and θ_2 are nonzero, and it is stable (unstable) at that point with a period of 2 if $\theta_2 > 0\,(<0)$.*

Proof. In a sufficiently small neighborhood with parameter $\delta = 0$, there exists a central manifold located at $(0,0)$:

$$W^c(0,0) = \left\{\left(\widetilde{N}_{n+1}, \widetilde{P}_{n+1}\right): \widetilde{P}_{n+1} = m_1\widetilde{N}_{n+1}^2 + m_2\widetilde{N}_{n+1}\delta\right\}. \tag{24}$$

Substituting (24) into (20), the solution is given as

$$\begin{aligned} m_1 &= \frac{e_{21}}{1-\lambda_2} = \frac{b_{21}k_{11}^2 + b_{22}k_{11}k_{21} + b_{23}k_{21}^2}{1-\lambda_2}, \\ m_2 &= \frac{-d_{21}}{1+\lambda_2} = \frac{-(a_{21}k_{11} + a_{22}k_{21})}{1+\lambda_2}. \end{aligned} \tag{25}$$

By focusing on the system of equations at $W^c(0,0)$, we can derive the following outcome:

$$\begin{aligned} \widetilde{N}_{n+1} = {} & -\widetilde{N}_n + r_1\widetilde{N}_n^2 + r_2\widetilde{N}_n\delta + r_3\widetilde{N}_n^2\delta + r_4\widetilde{N}_n\delta^2 \\ & + r_5\widetilde{N}_n^3 + O\left(\left(\left|\widetilde{N}_n\right| + |\delta|\right)^4\right), \end{aligned} \tag{26}$$

which $r_1 = e_{11} = b_{11}k_{11}^2 + b_{12}k_{11}k_{21} + b_{13}k_{21}^2$, $r_2 = d_{11} = a_{11}k_{11} + a_{12}k_{21}$, $r_3 = d_{12}m_1 + f_{11} + e_{12}m_2$, $r_4 = d_{12}m_2$, and $r_5 = e_{12}m_1 + e_{14}$.

Based on the reference [33], it is stated that when considering values at $(N, P, \delta) = (0,0,0)$ and having $\theta_1 \neq 0, \theta_2 \neq 0$, the system exhibits a flip bifurcation at the fixed point $N^*(x^*, y^*)$. *If* $\theta_2 > 0\,(<0)$, the point with a period of 2 is stable (unstable).

which

$$\begin{aligned} \theta_1 &= \left(\frac{\partial^2 f}{\partial\widetilde{N}_n\partial\delta} + \frac{1}{2}\frac{\partial f}{\partial\delta}\frac{\partial^2 f}{\partial\widetilde{N}_n^2}\right)\Bigg|_{(0,0)} = r_2, \\ \theta_2 &= \left(\frac{1}{6}\frac{\partial^3 f}{\partial\widetilde{N}_n^3} + \left(\frac{1}{2}\frac{\partial^2 f}{\partial\widetilde{N}_n^2}\right)^2\right)\Bigg|_{(0,0)} = r_5 + r_1^2. \end{aligned} \tag{27}$$

This completes the proof.

To validate the accuracy of the theoretical proof, numerical simulations are conducted in the following sections. When the parameters are taken as $h = 4.05937004, r = 0.8, d = 0.5, c = 0.9, b = 0.02, e = 0.6, a = 0.6, K = 9.99, m = 0.46$, (7) is satisfied; see Figure 3. □

Remark 6. From an ecological perspective, the occurrence of a flip bifurcation is characterized by population size fluctuating in cycles of 2, 4, 8, and so on until a chaotic state is reached. This phenomenon implies that prey populations cannot maintain stability, ultimately resulting in an ecological imbalance.

4. Hopf Bifurcation at Positive Equilibrium Point

4.1. Existence Conditions for Hopf Bifurcation. If a Hopf bifurcation occurs near a positive equilibrium point $N^*(x^*, y^*)$, the characteristic polynomial (3) must have a pair of conjugate unit complex roots. Consequently, we can deduce the bifurcation parameter as follows:

$$\lambda_1\lambda_2 = J_{11}(N^*) + J_{12}(N^*)J_{21}(N^*) = 1. \tag{28}$$

Since the step size $h > 0$, the choice of the bifurcation parameter under the condition $c\beta - ar > 0$, $\alpha > 0$ and $0 \le m < 1 - (br/\alpha(c\beta - ar))$ is given by

$$h_1^* = \frac{d_3}{d_4 d_5}, \tag{29}$$

where $d_3 = (2\alpha l^2/(1+\sqrt{\Delta})l^2 - Kbcr) - (2br/l) - (\beta(1-m)((\sqrt{\Delta}-1)l^2 - Kbcr)/2K(l + a(1-m)r)^2)$, $d_4 = (4K\alpha rl^3/(1+\sqrt{\Delta})l^2 - Kbcr) + (r/c)$, and $d_5 = (c\beta(1-m)((\sqrt{\Delta}-1)l^2 - Kbcr)/2K(l + a(1-m)r))$.

Taking δ as a small bifurcation parameter, i.e., $h = h_1^* + \delta$, $|\delta| \ll 1$. Then, characteristic (6) can be written as

$$\lambda^2 + s(\delta)\lambda + w(\delta) = 0, \tag{30}$$

in which $s(\delta) = -2 - (h_1^* + \delta)\mathrm{L}$, $w(\delta) = 1 + (h_1^* + \delta)\mathrm{L} + (h_1^* + \delta)^2((4K\alpha rl^3/i_2) + (r/c))((c\beta(1-m)i_1/i_3))$. The roots of the equation at $J|_{(x^*,y^*)}$ are

$$\lambda_1 = \frac{s(\delta) + i\sqrt{4w(\delta) - s(\delta)^2}}{2}, \lambda_2 = \frac{s(\delta) - i\sqrt{4w(\delta) - s(\delta)^2}}{2}, \tag{31}$$

in the meantime $|\lambda_{1,2}| = \sqrt{w(\delta)}(d|\lambda_{1,2}|/d\delta)\big|_{\delta=0} = (2i_3(\alpha l^3 - b\,i_2 r) + i_1 l\beta\,(1-m)(2h_1^* r(4\alpha cKl^3 + i_2) - i_2)/2\,i_2 i_3 l) \times (-Lh_1^* + (h_1^{*2} i_1 r\beta(1-m)\quad(4\alpha cKl^3 + i_2)/i_2 i_3) + 1)^{-(1/2)}$, $(d|\lambda_{1,2}|/d\delta)|_{\delta=0} \neq 0$ can be obtained if and only if $(2i_3(\alpha l^3 - bi_2 r) + i_1 l\beta(1-m)\,(2h_1^* r(4\alpha cKl^3 + i_2) - i_2)/2i_2 i_3 l) \neq 0$.

If $s(0) \neq 0, 1$, we have $-(h_1^* + \delta)L \neq 2, 3$, $\lambda_{1,2}^n \neq 1$, where $n = 1, 2, 3, 4$.

If $(d|\lambda_{1,2}|/d\delta)|_{\delta=0} \neq 0, -(h_1^* + \delta)L \neq 2, 3$, Hopf bifurcation occurs at the positive equilibrium point $N^*(x^*, y^*)$.

4.2. Normal Form of Hopf Bifurcation at Positive Equilibria. Assuming that $\lambda_1 = u + iv$, $\lambda_2 = u - iv$, where $u = (1/2)(-2 + h_1 L)$, $z = (4rh_1^2 i_1(4cKl^3\alpha)\beta(1-m)/i_2 i_3)$, $v = (1/2)\sqrt{4 - (2 - h_1 L)^2 + z - 4h_1 L}$. The corresponding invertible matrix can be obtained as

$$T = \begin{pmatrix} T_1 & T_2 \end{pmatrix} = \begin{pmatrix} -h^*\dfrac{4K\alpha rl^3}{i_2} + \dfrac{r}{c} & 0 \\ u - 1 - h^* L & -v \end{pmatrix}. \tag{32}$$

The corresponding inverse matrix is

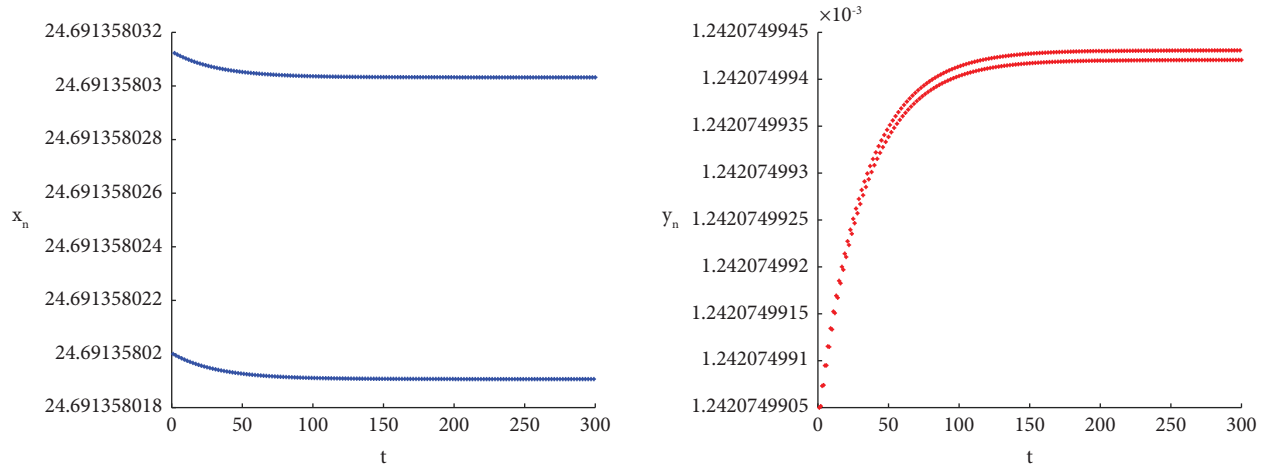

FIGURE 3: Flip bifurcation periodic solution at $N^*(x^*, y^*) = (24.691358, 0.001242)$ when the parameters are taken to be $h = 4.05937004, r = 0.8, d = 0.5, c = 0.9, b = 0.02, e = 0.6, a = 0.6, K = 9.99, m = 0.46$.

$$T^{-1} = \begin{pmatrix} \dfrac{ci_2}{ri_2 - 4cKl^3 r\alpha h^*} & 0 \\ \dfrac{ci_2(-1 + u - Lh^*)}{rv(i_2 - 4cKl^3\alpha h^*)} & -\dfrac{1}{v} \end{pmatrix}. \tag{33}$$

Using the following transformations $\begin{pmatrix} \overline{x_{n+1}} \\ \overline{y_{n+1}} \end{pmatrix} = T\begin{pmatrix} \overline{N_{n+1}} \\ \overline{P_{n+1}} \end{pmatrix}$, (10) is converted to

$$\begin{pmatrix} N_{n+1} \\ P_{n+1} \end{pmatrix} = \begin{pmatrix} u & -v \\ v & u \end{pmatrix}\begin{pmatrix} N_n \\ P_n \end{pmatrix} + \begin{pmatrix} \tilde{f}(\overline{N_n}, \overline{P_n}) \\ \tilde{g}(\overline{N_n}, \overline{P_n}) \end{pmatrix}, \tag{34}$$

in which

$$\begin{aligned} f(\overline{N_n}, \overline{P_n}) &= e_1\overline{N_n}^2 + e_2\overline{N_nP_n} + e_3\overline{P_n}^2 + e_4\overline{N_n}^3 + e_5\overline{N_n}^2\overline{P_n} + e_6\overline{N_nP_n}^2 + e_7\overline{P_n}^3, \\ g(\overline{N_n}, \overline{P_n}) &= s_1\overline{N_n}^2 + s_2\overline{N_nP_n} + s_3\overline{P_n}^2 + s_4\overline{N_n}^3 + s_5\overline{N_n}^2\overline{P_n} + s_6\overline{N_nP_n}^2 + s_7\overline{P_n}^3. \end{aligned} \tag{35}$$

The coefficients are

$$\begin{aligned} &e_1 = u^2z_1 + uvz_2 + v^2z_3, e_2 = -2uvz_1 + u^2z_2 - v^2z_2 + 2uvz_3, \\ &e_3 = v^2z_1 - uvz_2 + u^2z_3, e_4 = u^3z_4 + u^2vz_5 + uv^2z_6 + v^3z_7, \\ &e_5 = -3u^2vz_4 + u^3z_5 - 2uv^2z_5 + 2u^2vz_6 - v^3z_6 + 3uv^2z_7, \\ &e_6 = 3uv^2z_4 - 2u^2vz_5 + v^3z_5 + u^3z_6 - 2uv^2z_6 + 3u^2vz_7, \\ &e_7 = -v^3z_4 + uv^2z_5 - u^2vz_6 + u^3z_7, \\ &s_1 = u^2u_1 + uvu_2, s_2 = -2uvu_1 + u^2u_2 - v^2u_2, \\ &s_3 = v^2u_1 - uvu_2, s_4 = u^3u_3 + u^2vu_5, \\ &s_5 = -3u^2vu_3 + u^3u_5 - 2uv^2u_5, s_6 = 3uv^2u_3 - 2u^2vu_5 + v^3u_5, \\ &s_7 = v^3u_3 + uv^2u_5, \end{aligned} \tag{36}$$

so

$$\begin{pmatrix} \widetilde{f}(\overline{N_n}, \overline{P_n}) \\ \widetilde{g}(\overline{N_n}, \overline{P_n}) \end{pmatrix} = \begin{pmatrix} \dfrac{ci_2}{ri_2 - 4cKl^3 r\alpha h^*} & 0 \\ \dfrac{ci_2(-1+u-Lh^*)}{rv\left(i_2 - 4cKl^3\alpha h^*\right)} & -\dfrac{1}{v} \end{pmatrix} \begin{pmatrix} f(\overline{N_n}, \overline{P_n}) \\ g(\overline{N_n}, \overline{P_n}) \end{pmatrix}. \tag{37}$$

By utilizing the central manifold theorem and the normal form theory, we can determine the bifurcation direction of the Hopf bifurcation at the positive equilibrium point. Furthermore, by applying the canonical type theory of the Hopf bifurcation, we can evaluate the equation at $(\overline{N_n}, \overline{P_n}, \delta) = (0, 0, 0)$.

$$\begin{aligned}
M &= -Re\left[\frac{(1-2\lambda)\overline{\lambda}^2}{1-\lambda}\vartheta_{11}\vartheta_{20}\right] - \frac{1}{2}|\vartheta_{11}|^2 - |\vartheta_{02}|^2 + Re\left(\overline{\lambda}\vartheta_{21}\right), \\
\vartheta_{20} &= \frac{1}{8}\left(\widetilde{f}_{\overline{N_nN_n}} + \widetilde{f}_{\overline{P_nP_n}} + 2\widetilde{g}_{\overline{N_nP_n}} + i\left(\widetilde{g}_{\overline{N_nN_n}} - \widetilde{g}_{\overline{P_nP_n}} - 2\widetilde{f}_{\overline{N_nP_n}}\right)\right), \\
\vartheta_{11} &= \frac{1}{4}\left(\widetilde{f}_{\overline{N_nN_n}} + \widetilde{f}_{\overline{P_nP_n}} + i\left(\widetilde{g}_{\overline{N_nN_n}} + \widetilde{g}_{\overline{P_nP_n}}\right)\right), \\
\vartheta_{02} &= \frac{1}{8}\left(\widetilde{f}_{\overline{N_nN_n}} - \widetilde{f}_{\overline{N_nP_n}} + 2\widetilde{g}_{\overline{N_nP_n}} + i\left(\widetilde{g}_{\overline{N_nN_n}} - \widetilde{g}_{\overline{P_nP_n}} + 2\widetilde{f}_{\overline{N_nP_n}}\right)\right), \\
\vartheta_{21} &= \frac{1}{16}\left(\widetilde{f}_{\overline{N_nN_nN_n}} + \widetilde{f}_{\overline{N_nP_nP_n}} + \widetilde{g}_{\overline{N_nP_nP_n}} + \widetilde{g}_{\overline{P_nP_nP_n}} + i\left(\widetilde{g}_{\overline{N_nN_nN_n}} + \widetilde{g}_{\overline{N_nP_nP_n}} - \widetilde{f}_{\overline{N_nN_nP_n}} - \widetilde{f}_{\overline{P_nP_nP_n}}\right)\right), \\
\widetilde{f}_{\overline{N_nN_n}} &= 2\left(u^2z_1 + uvz_2 + v^2z_3\right), \widetilde{f}_{\overline{N_nP_n}} = -2uvz_1 + u^2z_2 - v^2z_2 + 2uvz_3, \\
\widetilde{f}_{\overline{N_nN_nP_n}} &= -6u^2vz_4 + 2u^3z_5 - 4uv^2z_5 + 4u^2vz_6 - 2v^3z_6 + 6uv^2z_7, \\
\widetilde{f}_{\overline{N_nP_nP_n}} &= 6uv^2z_4 - 4u^2vz_5 + 2v^3z_5 + 2u^3z_6 - 4uv^2z_6 + 6u^2vz_7, \\
\widetilde{f}_{\overline{P_nP_n}} &= 2v^2z_1 - 2uvz_2 + 2u^2z_3, \widetilde{f}_{\overline{P_nP_nP_n}} = -6v^3z_4 + 6uv^2z_5 - 6u^2vz_6 + 6u^3z_7, \\
\widetilde{g}_{\overline{N_nN_n}} &= 2u^2u_1 + 2uvu_2, \widetilde{g}_{\overline{N_nP_n}} = -2uvu_1 + u^2u_2 - v^2u_2, \\
\widetilde{g}_{\overline{N_nN_nN_n}} &= 6u^3u_3 + 6u^2vu_5, \widetilde{g}_{\overline{N_nN_nP_n}} = -6u^2vu_3 + 2u^3u_5 - 4uv^2u_5, \\
\widetilde{g}_{\overline{N_nP_nP_n}} &= 6uv^2u_3 - 4u^2vu_5 + 2v^3u_5, \widetilde{g}_{\overline{P_nP_n}} = 2v^2u_1 - 2uvu_2, \\
\widetilde{g}_{\overline{P_nP_nP_n}} &= 6v^3u_3 + 6uv^2u_5.
\end{aligned} \tag{38}$$

Theorem 7. *If $s(0) \neq 0, 1$ and $M \neq 0$, a Hopf bifurcation occurs at a positive equilibrium point $N^*(x^*, y^*)$. Moreover, if $M < 0$, an attracting invariant closed curve bifurcates from the equilibrium point for $\delta > 0$. On the other hand, if $M > 0$, a repelling invariant closed curve bifurcates from the equilibrium point for $\delta < 0$.*

To validate the accuracy of the theoretical proof, numerical simulations are conducted in the following sections. When the parameters are taken as $h = 0.168989, r = 0.2, K = 4.94, d = 0.8, c = 0.8, b = 0.01, e = 0.5, a = 0.5, m = 0.76$, (7) is satisfied; see Figure 4.

Remark 8. From an ecological perspective, as the parameter h approaches the critical value h^*, a stable curve emerges at the equilibrium point $N^*(x^*, y^*)$, indicating a stable coexistence between the prey and predator populations. Conversely, if the constant curve at the equilibrium point $N^*(x^*, y^*)$ becomes unstable as h increases, the populations of prey and predators will fail to reach a stable state, leading to an ecological imbalance within the ecosystem.

5. Chaotic Analysis

In general, flip bifurcation and Hopf bifurcation are two ways in which discrete systems move towards chaos. Under

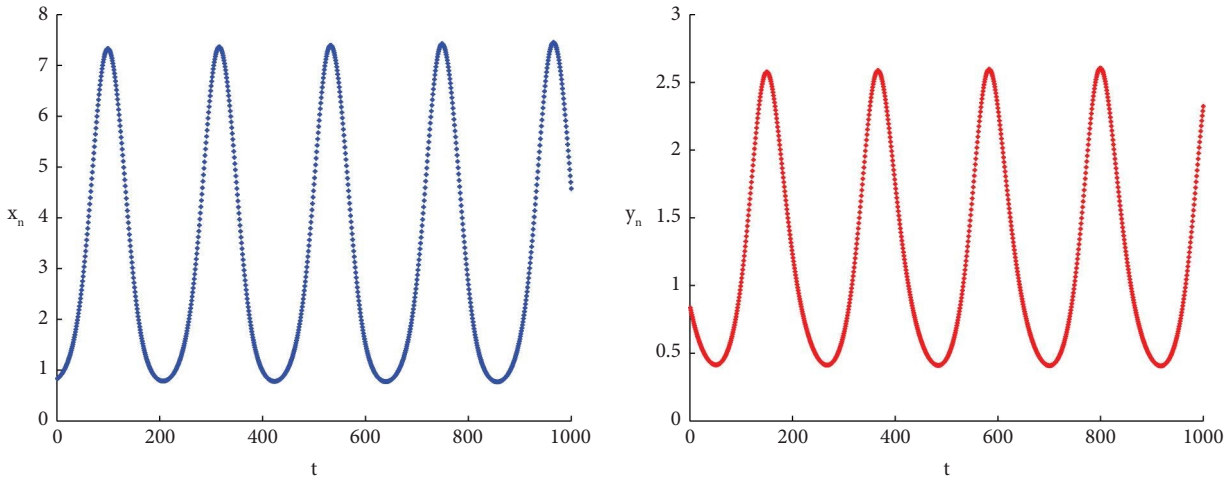

FIGURE 4: Hopf bifurcation periodic solution at $N^*(x^*, y^*) = (0.83333, 0.83595)$ when the parameters are taken to be $h = 0.168989, r = 0.2, K = 4.94, d = 0.8, c = 0.8; b = 0.01, e = 0.5, a = 0.5, m = 0.76$.

the condition of the existence of two kinds of bifurcations, applying perturbations to the bifurcation parameters, sometimes a chaotic situation occurs, which is discussed in the following.

5.1. Existence of Chaos

Definition 9 (see [34]). For the system $x_{n+1} = f(x_n)$, $y_{n+1} = f(y_n)$, if a small perturbation is applied to the system, the system will diverge as the number of iterations increases, and the degree of divergence is usually expressed using the maximum Lyapunov index, which is given by

$$\lambda = \lim_{n\longrightarrow\infty} \frac{1}{k} \sum_{n=0}^{n-1} \ln\left|\frac{df(x_n, \mu)}{dx}\right|. \tag{39}$$

Theorem 10 (see [34]). *If $\lambda < 0$, it is an indication that neighboring points will eventually converge to a single point. This is the equivalent of stable, motionless points and periodic motion. On the other hand, if $\lambda > 0$, it means that neighboring points will eventually separate from each other. This means that orbits are locally unstable and chaotic.*

After selecting the perturbation $\delta = (0, 1.5)$, the trend of x is analyzed numerically, and through numerical simulation, the maximum Lyapunov exponential map agrees with the trend of the bifurcation map, see Figures 5–7.

5.2. Chaos Control. Using the state feedback control method [35–37] to stabilize the chaotic orbit at an unstable equilibrium point of the system (3) and to achieve this, we introduce the following controlled system, which corresponds to (3):

$$\begin{cases} x_{n+1} = x_n + h\left(\dfrac{\alpha x_n}{1 + Ky_n} - bx_n^{\,2} - \dfrac{\beta(1-m)x_n y_n}{1 + a(1-m)x_n}\right) - U_n, \\ y_{n+1} = y_n + h\left(-ry_n + \dfrac{c\beta(1-m)x_n y_n}{1 + a(1-m)x_n}\right). \end{cases} \tag{40}$$

The feedback control is defined as $U_n = \sigma(x_n - x^*) + \theta(y_n - y^*)$, where σ and θ are the feedback gains and $N^*(x^*, y^*)$ represents the only positive equilibrium point of the system.

The Jacobi matrix of the controlled system at the exclusive positive equilibrium point is displayed underneath:

$$F_J(x^*, y^*) = \begin{pmatrix} J_{11} - \sigma & J_{12} - \theta \\ J_{21} & J_{22} \end{pmatrix}, \tag{41}$$

where $J_{11} = 1 + h((\alpha/1 + Ky^*) - 2bx^* - (\beta(1-m)y^*/(1 + a(1-m)x^*)^2))$, $J_{12} = -h((K\alpha x^*/(1 + Ky^*)^2) + (\beta(1-m)x^*/1 + a(1-m)x^*))$, $J_{21} = (hc\beta(1-m)y^*/(1 + a\ (1-m)x^*)^2)$, $J_{22} = 1 + h(-r + (c\beta(1-m)x^*/1 + a\ (1-m)x^*))$.

From the Jacobi matrix, the corresponding characteristic equation is

$$\lambda^2 - (J_{11} + J_{22} - \sigma)\lambda + J_{22}(J_{11} - \sigma) - J_{21}(J_{12} - \theta) = 0. \tag{42}$$

Let λ_1, λ_2 be the two eigenvalues of the equation, which gives

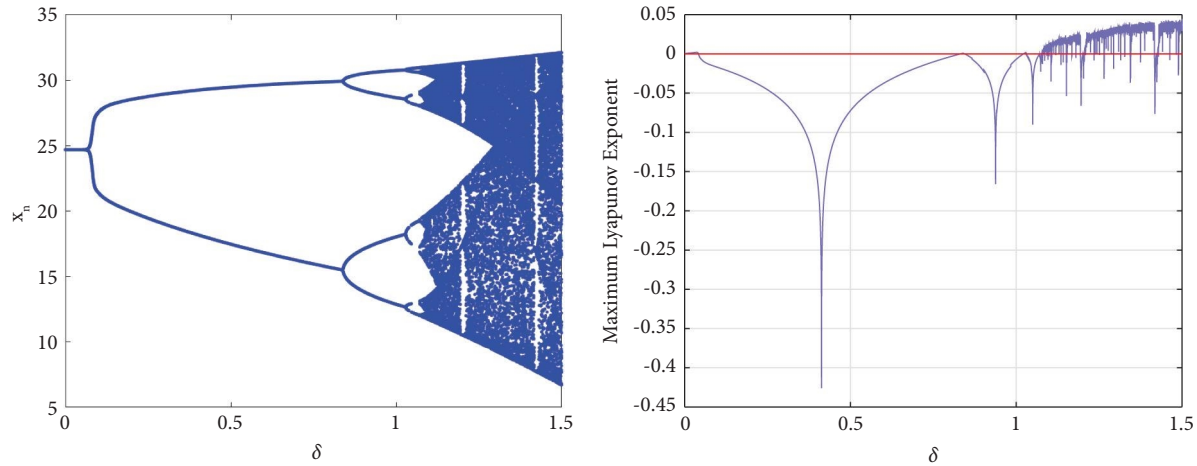

FIGURE 5: Flip bifurcation diagrams and MLE at $N^*(x^*, y^*) = (24.69135.001242)$ for system (3) with $h = 4.05937, r = 0.8, d = 0.5, c = 0.9, b = 0.02, e = 0.6, a = 0.6, K = 9.99, m = 0.46$.

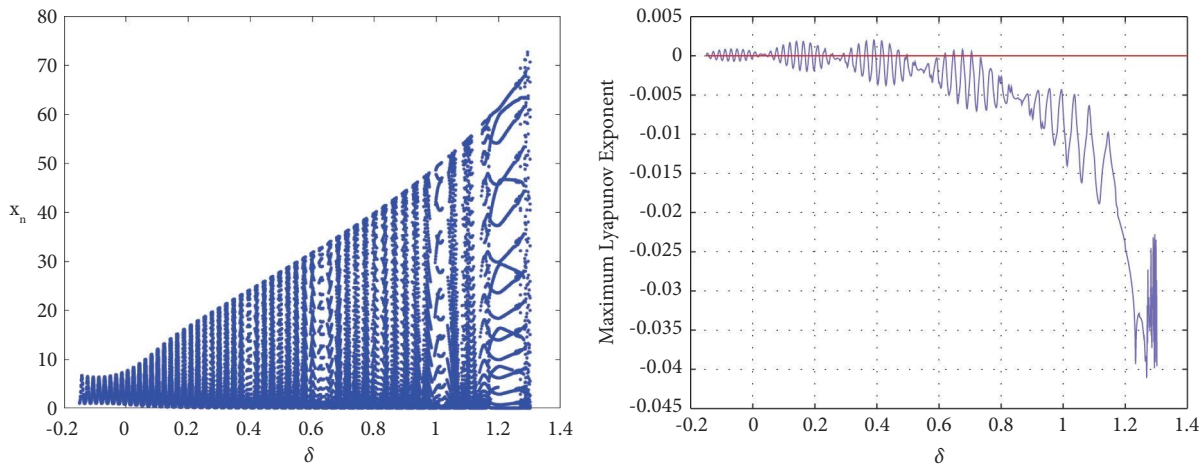

FIGURE 6: Hopf bifurcation diagrams and MLE at $N^*(x^*, y^*) = (0.83333, 0.83595)$ for system (3) with $h = 0.1689893, r = 0.2, K = 4.94, d = 0.8, c = 0.8, b = 0.01, e = 0.5, a = 0.5, m = 0.76$.

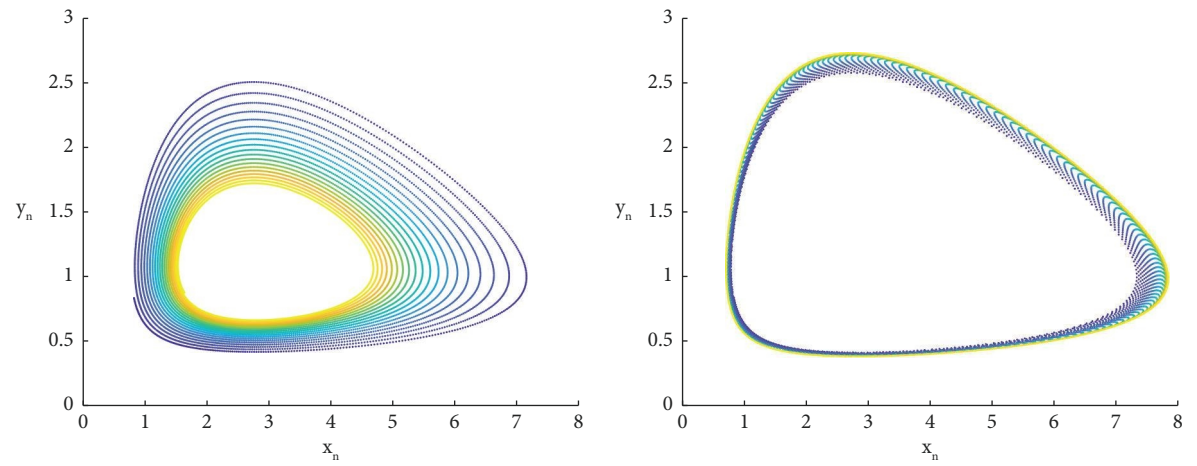

FIGURE 7: Continued.

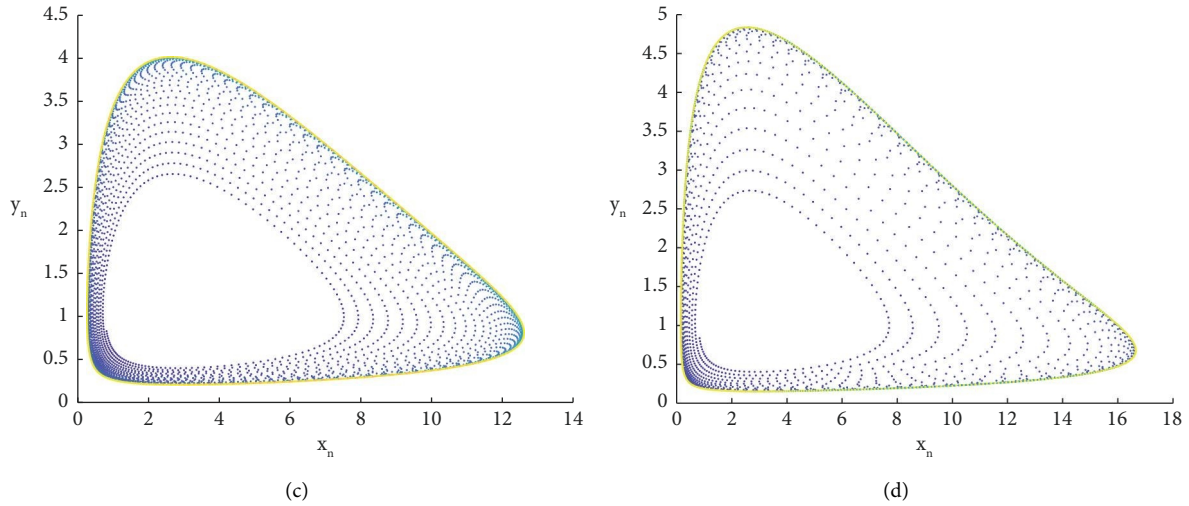

FIGURE 7: Phase diagrams in the presence of different perturbations δ at the equilibrium point $N^*(x^*, y^*)$. (a) $\delta = -0.1$. (b) $\delta = 0$. (c) $\delta = 0.1$. (d) $\delta = 0.2$.

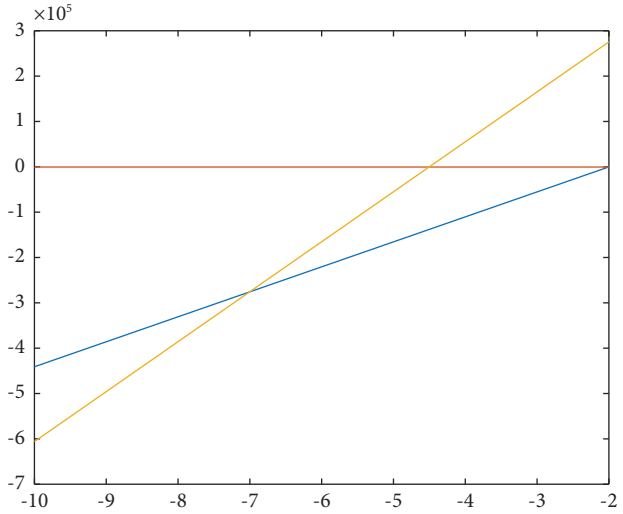

FIGURE 8: Flip bifurcation stabilization regions of system (3) at $h = 4.05937004, r = 0.8, d = 0.5, c = 0.9, b = 0.02, e = 0.6, a = 0.6, K = 9.99, m = 0.46$.

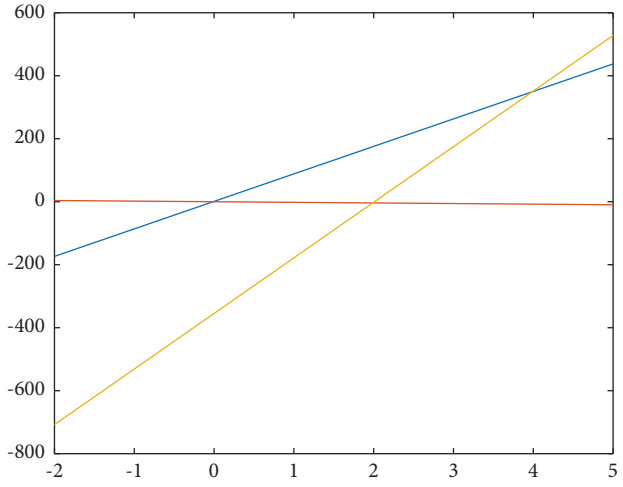

FIGURE 9: Hopf bifurcation stabilization regions of system (3) at $h = 0.1689893, r = 0.2, K = 4.94, d = 0.8, c = 0.8, b = 0.01, e = 0.5, a = 0.5, m = 0.76$.

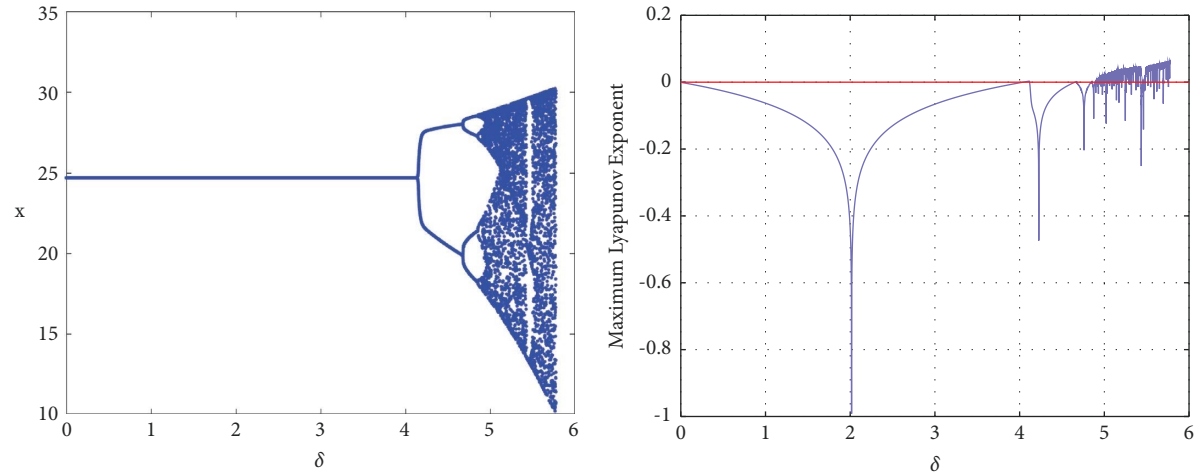

(a) (b)

Figure 10: Flip bifurcation diagrams and MLE for system (3) with $h = 4.05937, r = 0.8, d = 0.5, c = 0.9, b = 0.02, e = 0.6, a = 0.6, K = 9.99, m = 0.46$ and initial conditions $\sigma = -2, \theta = 0$.

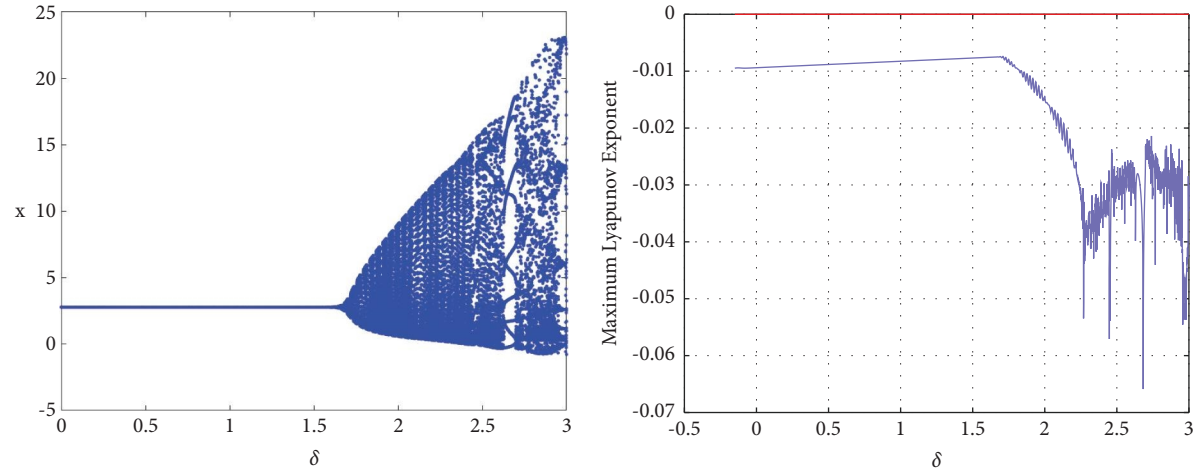

(a) (b)

Figure 11: Hopf bifurcation diagrams and MLE for system (3) with $h = 0.1689893, r = 0.2, K = 4.94, d = 0.8, c = 0.8, b = 0.01, e = 0.5, a = 0.5, m = 0.76$ and initial conditions $\sigma = 0.1, \theta = -0.01$.

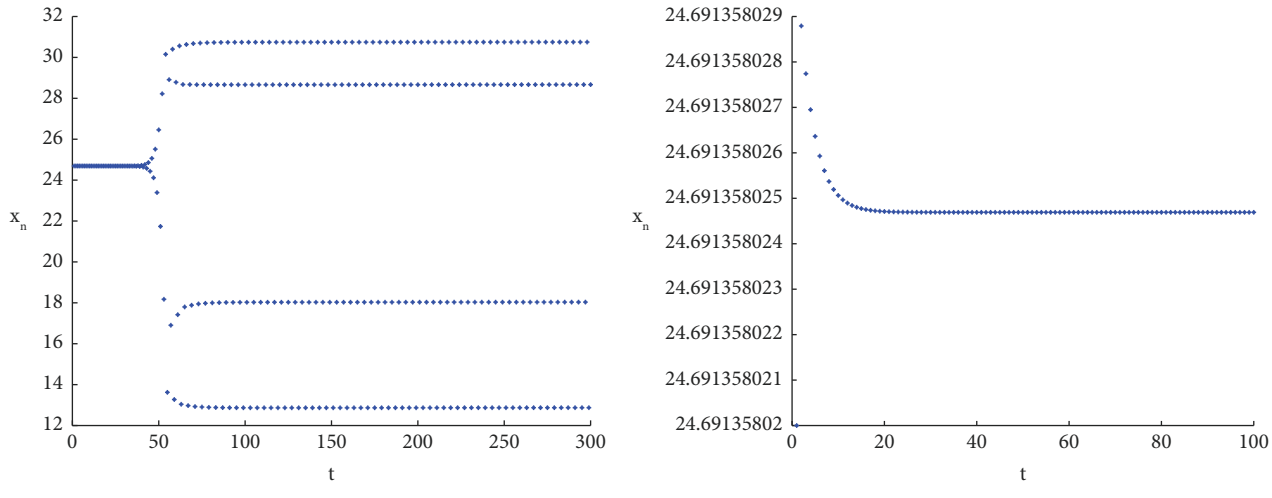

(a) (b)

Figure 12: Continued.

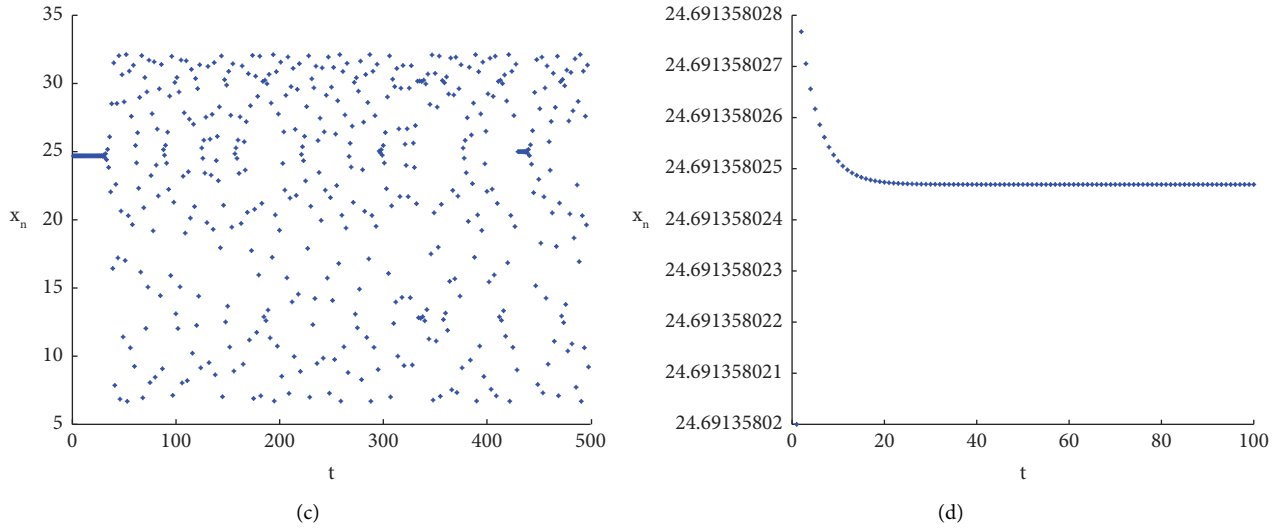

FIGURE 12: Changes in prey population size over time when different values of perturbation δ are taken. Here, a, b is the case where the perturbation δ is 1 before and after control, and c, d is the case where the perturbation δ is 1.5 before and after control. (a) Before control $\delta = 1$. (b) After control, $\delta = 1$. (c) Before control, $\delta = 1.5$. (d) After control, $\delta = 1.5$.

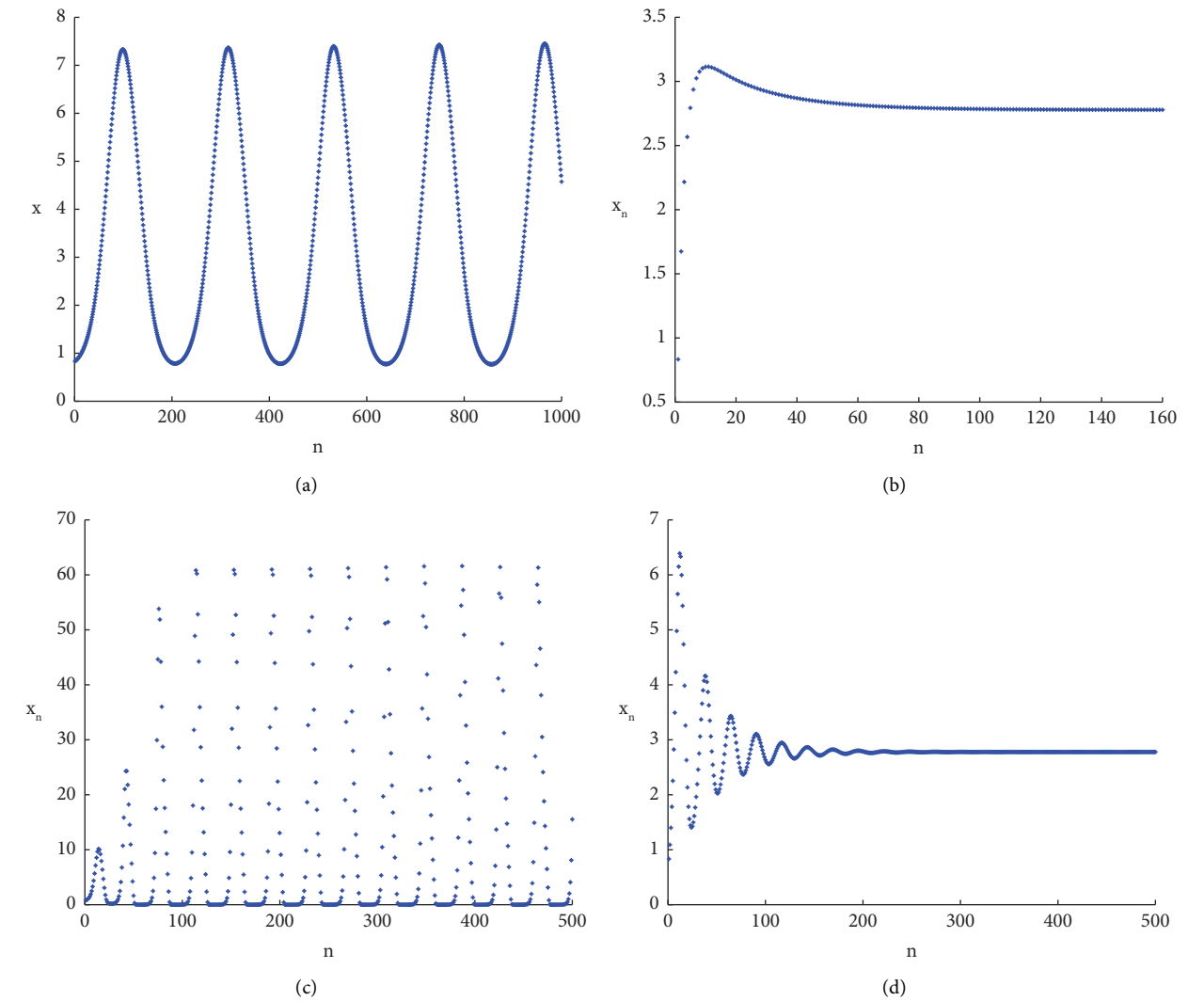

FIGURE 13: Changes in prey population size over time when different values of perturbation δ are taken. Where a, b is the case where the perturbation δ is 0 before and after control, and c, d is the case where the perturbation δ is 1.2 before and after control. (a) Before control, $\delta = 0$. (b) After control, $\delta = 0$. (c) Before control, $\delta = 1.2$. (d) After control, $\delta = 1.2$.

$$\lambda_1 + \lambda_1 = J_{11} + J_{22} - \sigma, \lambda_1\lambda_2 = J_{22}(J_{11} - \sigma) - J_{21}(J_{12} - \theta). \tag{43}$$

To determine the lines of marginal stability, we need to solve the equations $\lambda_1 = \pm 1$ and $\lambda_1\lambda_2 = 1$. These equations impose constraints that guarantee the absolute values of λ_1 and λ_2 are both less than 1. By finding the solutions to these equations, we can identify the boundaries of stability.

Assume that $\lambda_1\lambda_2 = 1$, it is possible to obtain L_1: $J_{11}J_{22} - J_{21}J_{12} - 1 = \sigma J_{22} - \theta J_{21}$.

Next, assuming $\lambda_1 = 1$, one obtains L_2: $\sigma(1 - J_{22}) + \theta J_{21} = J_{11} + J_{22} - 1 - J_{11}J_{22} + J_{21}J_{12}$.

Assuming $\lambda_1 = -1$, one obtains L_3: $\sigma(1 + J_{22}) - \theta J_{21} = J_{11} + J_{22} + 1 + J_{11}J_{22} - J_{21}J_{12}$.

It is evident that, for specific parameter values, the stable eigenvalues are situated within the triangular region defined by the straight lines L_1, L_2, L_3; see Figures 8 and 9. By selecting the appropriate parameter values in the restricted area, it becomes apparent that the perturbation values increase significantly when chaos emerges within the controlled region;, see Figures 10 and 11. Furthermore, the temporal evolution of the population numbers, both before and after implementing control measures, can be effectively validated through visual representations; see Figures 12 and 13.

Remark 11. From the ecological point of view, when unfavourable chaos occurs, the antidisturbance ability of the ecosystem is greatly enhanced by carrying out chaos control, which is conducive to maintaining the stability of the ecosystem and reducing the problem of ecological imbalance. As an example, greening and the establishment of biological shelters can effectively reduce the state of chaos among groups of organisms, thus effectively protecting and managing the diversity of species.

6. Conclusion

In this paper, we investigate a discrete predator-prey model incorporating fear effects and refuge. We begin by discussing the local stability and instability conditions of the three equilibrium points of system (3). Specifically, we analyze the occurrence of flip bifurcation at eigenvalues $|\lambda_1| = -1$ and $|\lambda_2| < 1$ of characteristic (6). Additionally, we explore the Hopf bifurcation that arises when the eigenvalues of characteristic (6) form a pair of conjugate unit complex roots. We also examine the bifurcation directions associated with these two types of bifurcations.

The chaotic behavior of the system is investigated through both theoretical proofs and numerical simulations. We demonstrate that chaotic dynamics can be controlled using the feedback control method. Bifurcation diagrams and maximum Lyapunov exponent diagrams clearly illustrate the significant increase in perturbation values when system (3) exhibits chaos after control.

From a biological perspective, the stability analysis of the equilibrium points reveals that, under the influence of fear and other factors, the predator and prey populations eventually reach an equilibrium state, allowing for harmonious coexistence. By controlling the chaotic situations arising from flip and Hopf bifurcations, we can effectively suppress chaotic behavior among organisms. This can be achieved through various human-imposed interventions such as greening, establishing biological refuges, and implementing other measures. These interventions are beneficial for the survival and development of biological populations.

In future research, it would be worthwhile to explore different chaos control methods in order to achieve improved control effects.

Data Availability

No data were used to support the findings of this study.

Conflicts of Interest

The authors declare that they have no conflicts of interest.

Authors' Contributions

The idea of this research was introduced by W. Li. All the authors contributed to the main results and numerical simulations. C. Zhang and M Wang contributed to revising the manuscript.

Acknowledgments

This research was supported by the Fundamental Research Funds for the Central Universities (no. 60201523050).

References

[1] J. Wang, Y. Cai, S. Fu, and W. Wang, "The effect of the fear factor on the dynamics of a predator-prey model incorporating the prey refuge," *Chaos*, vol. 29, no. 8, Article ID 83109, 2019.

[2] M. A. Aziz-Alaoui and M. Daher Okiye, "Boundedness and global stability for a predator-prey model with modified Leslie-Gower and Holling-type II schemes," *Applied Mathematics Letters*, vol. 16, no. 7, pp. 1069–1075, 2003.

[3] S. Li and W. Zhang, "Bifurcations of a discrete prey-predator model with Holling type II functional response," *Discrete & Continuous Dynamical Systems- B*, vol. 14, no. 1, pp. 159–176, 2010.

[4] A. N. W. Hone, M. V. Irle, and G. W. Thurura, "On the Neimark-Sacker bifurcation in a discrete predator-prey system," *Journal of Biological Dynamics*, vol. 4, no. 6, pp. 594–606, 2010.

[5] L. A. D. Rodrigues, D. C. Mistro, and S. Petrovskii, "Pattern formation, long-term transients, and the Turing-Hopf bifurcation in a space-and time-discrete predator-prey system," *Bulletin of Mathematical Biology*, vol. 73, no. 8, pp. 1812–1840, 2011.

[6] S. V. Petrovskii, A. Y. Morozov, and E. Venturino, "Allee effect makes possible patchy invasion in a predator-prey system," *Ecology Letters*, vol. 5, no. 3, pp. 345–352, 2002.

[7] X. Zhang, C. Zhang, and Y. Zhang, "Pattern dynamics analysis of a time-space discrete FitzHugh-Nagumo(FHN) model based on coupled map lattices," *Computers and Mathematics*

with Applications&Mathematics with Applications, vol. 157, pp. 92–123, 2024.

[8] T. Li, X. Zhang, and C. Zhang, "Pattern dynamics analysis of a space-time discrete spruce budworm model," *Chaos, Solitons and Fractals*, vol. 179, Article ID 114423, 2024.

[9] V. G. Ivancevic, T. T. Ivancevic, Z. Liang, S. He, H. Wang, and K. Sun, "Complex nonlinearity: chaos, phase transitions, topology change and path integrals," *The European Physical Journal Plus*, vol. 137, no. 3, p. 303, 2022.

[10] C. S. Bertuglia and F. Vaio, *Nonlinearity, Chaos, and Complexity: The Dynamics of Natural and Social Systems*, Oxford University Press, Oxford, UK, 2005.

[11] C. Lei, X. Han, and W. Wang, "Bifurcation analysis and chaos control of a discrete-time prey-predator model with fear factor," *Mathematical Biosciences and Engineering*, vol. 19, no. 7, pp. 6659–6679, 2022.

[12] X. S. Luo, G. Chen, B. Hong Wang, and J. Qing Fang, "Hybrid control of period-doubling bifurcation and chaos in discrete nonlinear dynamical systems," *Chaos, Solitons and Fractals*, vol. 18, no. 4, pp. 775–783, 2003.

[13] A. Singh and V. S. Sharma, "Bifurcations and chaos control in a discrete-time prey-predator model with Holling type-II functional response and prey refuge," *Journal of Computational and Applied Mathematics*, vol. 418, Article ID 114666, 2023.

[14] S. Akhtar, R. Ahmed, M. Batool, N. A. Shah, and J. D. Chung, "Stability, bifurcation and chaos control of a discretized Leslie prey-predator model," *Chaos, Solitons and Fractals*, vol. 152, Article ID 111345, 2021.

[15] S. M. Salman, A. M. Yousef, and A. A. Elsadany, "Stability, bifurcation analysis and chaos control of a discrete predator-prey system with square root functional response," *Chaos, Solitons and Fractals*, vol. 93, pp. 20–31, 2016.

[16] A. Hastings and T. Powell, "Chaos in a three-species food chain," *Ecology*, vol. 72, no. 3, pp. 896–903, 1991.

[17] R. M. May, "Biological populations with nonoverlapping generations: stable points, stable cycles, and chaos," *Science*, vol. 186, no. 4164, pp. 645–647, 1974.

[18] S. Vinoth, R. Sivasamy, and K. Sathiyanathan, "A novel discrete-time Leslie-Gower model with the impact of Allee effect in predator population," *Complexity*, p. 2022, 2022.

[19] A. Arsie, C. Kottegoda, and C. Shan, "A predator-prey system with generalized Holling type IV functional response and Allee effects in prey," *Journal of Differential Equations*, vol. 309, pp. 704–740, 2022.

[20] S. Vinoth, R. Sivasamy, K. Sathiyanathan et al., "The dynamics of a Leslie type predator-prey model with fear and Allee effect," *Advances in Difference Equations*, vol. 2021, pp. 338–422, 2021.

[21] A. R. M. Jamil and R. K. Naji, "Modeling and analysis of the influence of fear on the Harvested modified Leslie-Gower model Involving nonlinear prey refuge," *Mathematics*, vol. 10, no. 16, p. 2857, 2022.

[22] N. D. Kazarinoff and P. Van Den Driessche, "A model predator-prey system with functional response," *Mathematical Biosciences*, vol. 39, no. 1-2, pp. 125–134, 1978.

[23] J. Wang, J. Shi, and J. Wei, "Predator-prey system with strong Allee effect in prey," *Journal of Mathematical Biology*, vol. 62, no. 3, pp. 291–331, 2011.

[24] P. Auger, R. Mchich, T. Chowdhury, G. Sallet, M. Tchuente, and J. Chattopadhyay, "Effects of a disease affecting a predator on the dynamics of a predator-prey system," *Journal of Theoretical Biology*, vol. 258, no. 3, pp. 344–351, 2009.

[25] R. Cressman and J. Garay, "A predator-prey refuge system: evolutionary stability in ecological systems," *Theoretical Population Biology*, vol. 76, no. 4, pp. 248–257, 2009.

[26] Z. Ma, W. Li, Y. Zhao, W. Wang, H. Zhang, and Z. Li, "Effects of prey refuges on a predator-prey model with a class of functional responses: the role of refuges," *Mathematical Biosciences*, vol. 218, no. 2, pp. 73–79, 2009.

[27] F. S. Berezovskaya, B. Song, and C. Castillo-Chavez, "Role of prey dispersal and refuges on predator-prey dynamics," *SIAM Journal on Applied Mathematics*, vol. 70, no. 6, pp. 1821–1839, 2010.

[28] H. Qi and X. Meng, "Threshold behavior of a stochastic predator-prey system with prey refuge and fear effect," *Applied Mathematics Letters*, vol. 113, Article ID 106846, 2021.

[29] X. Wang, L. Zanette, and X. Zou, "Modelling the fear effect in predator-prey interactions," *Journal of Mathematical Biology*, vol. 73, no. 5, pp. 1179–1204, 2016.

[30] N. H. Fakhry and R. K. Naji, "The dynamics of a square root prey-predator model with fear," *Iraqi Journal of Science*, pp. 139–146, 2020.

[31] H. Zhang, Y. Cai, S. Fu, and W. Wang, "Impact of the fear effect in a prey-predator model incorporating a prey refuge," *Applied Mathematics and Computation*, vol. 356, pp. 328–337, 2019.

[32] X. Liu and D. Xiao, "Complex dynamic behaviors of a discrete-time predator-prey system," *Chaos, Solitons and Fractals&Fractals*, vol. 32, no. 1, pp. 80–94, 2007.

[33] B. Hong and C. Zhang, "Bifurcations and chaotic behavior of a predator-prey model with discrete time," *AIMS Mathematics*, vol. 8, no. 6, pp. 13390–13410, 2023.

[34] L. M. Pecora and T. L. Carroll, "Synchronization in chaotic systems," *Physical Review Letters*, vol. 64, no. 8, pp. 821–824, 1990.

[35] S. Elaydi, *An Introduction to Difference Equations*, Springer-Verlag, New York, NY, USA, 3rd edition, 2005.

[36] S. Lynch, *Dynamical Systems with Applications Using Mathematica*, Birkhäuser, Boston, MA, USA, 2007.

[37] G. Chen and X. Dong, "From chaos to order: methodologies, perspectives and applications," *Methodologies Perspectives Applications*, World Scientific, Singapore, 1998.